

**LABORATORY SIMULATIONS OF SOLAR WIND ION IRRADIATION ON THE SURFACE OF MERCURY.** C. Bu<sup>1\*</sup>, B. C. Bostick<sup>2</sup>, S. N. Chillrud<sup>2</sup>, D. L. Domingue<sup>3</sup>, D. S. Ebel<sup>4</sup>, G. E. Harlow<sup>4</sup>, R. M. Killen<sup>5</sup>, D. Schury<sup>1</sup>, K. P. Bowen<sup>1</sup>, P.-M. Hillenbrand<sup>1</sup>, X. Urbain<sup>6</sup>, R. Zhang<sup>1</sup>, and D. W. Savin<sup>1</sup>. <sup>1</sup>Columbia Astrophysics Laboratory, Columbia University, New York, NY 10027 (\*[Caixia.Bu@columbia.edu](mailto:Caixia.Bu@columbia.edu); [dws26@columbia.edu](mailto:dws26@columbia.edu)). <sup>2</sup>Lamont-Doherty Earth Observatory, Columbia University, Palisades, NY 10964. <sup>3</sup>Planetary Science Institute, Tucson, AZ 85719. <sup>4</sup>American Museum of Natural History, New York, NY 10024. <sup>5</sup>NASA-Goddard Space Flight Center, Greenbelt, MD 20771. <sup>6</sup>Université Catholique de Louvain, B-1348 Louvain-la-Neuve, Belgium.

**Introduction:** Na and He are the two dominant confirmed neutral species in the Hermean exosphere. Studies of the Na exosphere provide clues to the surface mineralogy and are an important constraint for formation models of Mercury. The solar wind is the source of the He, while the Na source is predicted to be plagioclase feldspars on Mercury's surface [1, 2]. Observations from the ground [3, 4] and from the MESSENGER mission [5, 6] find variable enhanced high latitude Na abundance in Mercury's exosphere, suggesting that the Na is due to sputtering by solar wind ions precipitating to the surface through the planet's magnetic cusps. A number of models have been developed to explain the Na exosphere [7, 8]. However, the models make questionable assumptions about the sputter yield from ion irradiation, due to the lack of experimental data for regolith-like loose powders.

Spectrophotometry is a combined analysis of the spectral and photometric properties of a surface [9], enabling understanding composition and regolith structure. MESSENGER's MACSC and MDIS instruments provided spectral and photometric observations. However, to better interpret these observations, we need to understand how solar wind ions affect the spectrophotometry of Na-bearing minerals such as plagioclase feldspars, which are inferred to be abundant on Mercury's surface [1].

We plan to perform ion-irradiation studies on loose powder analogs of Mercury's regolith, with the aim of providing quantitative data for the corresponding sputtering yields and spectrophotometric changes. Our goal is to improve the interpretation of *in-situ* and remote-sensing data of Mercury through benchmark laboratory studies.

**Experimental Methods:** We are commissioning a novel ion-beam apparatus to simulate solar wind ion irradiation of regolith analogs (Fig. 1). The ion beam is generated using a duoplasmatron [10], horizontally accelerated to energies of 1 – 20 keV, and a Wien filter used to select the desired charge-to-mass ion. The ion beam next passes through a series of ion optics, an electrostatic bender (deflecting the beam downward and preventing ultraviolet light and neutrals from the source from reaching the samples), through another series of

ion optics, and then two apertures (constraining the beam divergence to  $\pm \sim 0.14^\circ$ ). The ions impact the target samples inside the target chamber at a polar angle  $\theta = 45^\circ$  measured relative to the bulk normal and irradiation area of  $\sim 1 \text{ cm}^2$ . The pressure at the ion source is  $\sim 1 \times 10^{-6}$  Torr,  $\sim 1 \times 10^{-8}$  Torr along the beam line, and  $\sim 5 \times 10^{-10}$  Torr in the target chamber.

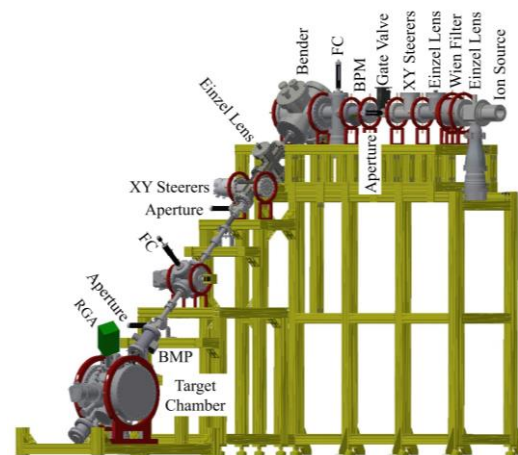


Fig. 1. Schematic of the experimental apparatus for ion irradiation of regolith-like loose powder samples.

**Ion irradiation.** To simulate solar wind ions, we will use beams of 1 keV  $\text{H}^+$  and 4 keV  $\text{He}^+$ , with fluxes of  $\sim 6 \times 10^{11}$  and  $3 \times 10^{13}$  ions  $\text{cm}^{-2} \text{ s}^{-1}$ , respectively. Fluences will be achieved of  $\sim 10^{17}$  ions  $\text{cm}^{-2}$  for  $\text{H}^+$  in 48 hrs and of  $10^{18}$  ions  $\text{cm}^{-2}$  for  $\text{He}^+$  in 9 hrs. During ion irradiation, the ion beam shape and current will be monitored by a beam profile monitor (BPM) [11], which has been calibrated by a retractable Faraday Cup (FC) before the sample. As the samples have insulating properties, we will use an electron flood gun ( $\sim \text{eV}$  energies) to neutralize sample surface charging.

**Samples.** Plagioclase feldspar is inferred to be the carrier of Na in the surface lavas of Mercury and thereby the source of the planet's Na exosphere. For our ion-irradiation samples, we will use gem quality Na-bearing feldspar. One of the main features of the apparatus is that samples in the target chamber are held horizontally (Fig. 2), enabling us to ion irradiate regolith-like loose powders. The samples will be ground and dry sieved into size fractions of 20 – 40, 40 – 70, and 70 – 120  $\mu\text{m}$ .

After mounting the sample in the target chamber, we will heat the chamber to 100°C for 24 – 48 hrs in vacuum, to thermally desorb sample surface contaminants (H<sub>2</sub>O, O<sub>2</sub>, CO<sub>2</sub>, etc.). Prior to the studies using mineral samples, we will perform proof-of-principle sputter yield measurements with a pure copper slab target and 20 keV Kr<sup>+</sup>.

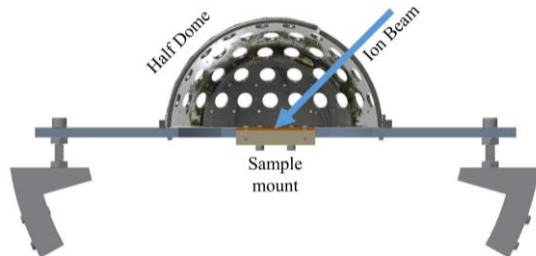


Fig.2 Schematic of the sample mount and the half dome holding the catcher foils. The foils are located at the openings in the half dome, not all of which are visible here. The structure mounts onto the inner walls of the target chamber using the arc-shaped feet.

*Sputter yield and its angular and energy distributions.* Sputtered particles will be collected by catcher foils mounted on a half dome (radius = 7 cm) surrounding the sample (Fig. 2). The catcher foils are gold-coated quartz crystals, and the effective collecting area of each foil is 0.8 cm<sup>2</sup>. There is one foil at a polar angle  $\theta = 0^\circ$ , 4 at  $15^\circ$ , 6 at  $30^\circ$ , 8 at  $45^\circ$ , 10 at  $60^\circ$ , and 12 at  $75^\circ$ . The azimuthal angles  $\phi$  ranging from  $0^\circ$  to  $180^\circ$ . The ion beam direction is defined as  $\theta = 45^\circ$  and  $\phi = 0^\circ$ . To determine the angular distribution of the total yield of sputtered particles on an absolute scale, we will perform quartz crystal microbalance (QCM) mass-gain measurements on each of the foils before and after each ion-irradiation experiment, using a high precision, trace metal clean, automated weighing system with a HEPA-filtered environmentally controlled chamber. The buoyancy corrected QCM method provides absolute mass-gain measurements to within 0.5  $\mu\text{g}$ . We will also analyze the foils *ex-situ* using synchrotron based X-ray photoelectron spectroscopy (XPS) to determine relative elemental abundances for the sputtered particles. The XPS spectra vs. X-ray energy will provide a depth profile of the relative elemental abundances of the sputtered particles on each foil, which can be used to determine the relative elemental sputter yields and the energy distribution of the sputtered particles.

*In-situ bidirectional reflectance measurements.* The target chamber is designed with appropriate ports, so that we can perform *in-vacuo* and *in-situ* 350 – 2500 nm spectroscopic analyses as a function of ion fluence. Spectra will be collected using a tungsten halogen light source and an Analytical Spectra Devices LabSpec 4

spectrometer. An ultra-high vacuum compatible optical fiber system is used to direct the light from source to the sample, and another to collect the reflected light and direct it into the spectrometer. Spectra will be collected for incidence and emergent angles spanning  $-45^\circ$  to  $+45^\circ$ , covering phase angles from  $15^\circ$  to  $90^\circ$ . The fiber cables lie in a plane that is offset by a polar angle  $\theta = 15^\circ$  to prevent any issue with specular reflectance. Spectralon reflectance standards will be used.

**Current Status and Plans:** We have completed the construction of the ion-irradiation apparatus and are now calibrating the measurement system for ion fluence. We have also completed the design and construction of sample stage and the half dome with catcher foils (Fig. 2). Our next step is to align the target chamber and half dome system with the ion beam trajectory. Then we will begin performing the proof-of-principle sputtering measurement, to be followed with measurements using powders of feldspar.

**Conclusions:** We are commissioning a novel ion-irradiation apparatus that allows us to simulate solar-wind ion irradiation on Mercury, as well as other planetary surfaces, using regolith-like loose powders. We also have designed a system to collect the ion-induced sputtered particles using catch foils. By analyzing the mass gain and stoichiometry of the sputtered atoms on the foils, we will be able to derive the absolute elemental sputter yields and their angular and energy distributions. The system will also enable *in-situ* bidirectional reflectance spectral analysis as a function of ion fluence. The laboratory measured sputter yields and spectral changes will be incorporated into current exosphere and spectrophotometric models to improve our understanding of Mercury's exosphere and surface compositions.

**Acknowledgments:** We acknowledge support, in part, from a NASA Solar System Workings Program Award No. 80NSSC18K0521 and an NIH award No. 1S10OD016219.

**References:** [1] T. J. McCloy et al. (2018), in *The View after MESSENGER*, 176–190. [2] W. E. McClintock et al. (2018), in *The View after MESSENGER*, 371–406. [3] A. E. Potter et al. (1999) *Space Sci.* 47, 1441–1448. [4] A. E. Potter et al. (2002) *Planet. Sci.* 37, 1165–1172. [5] R. J. Vervack et al. (2010) *Science* 329, 672–675. [6] V. Mangano et al. (2015) *Planet. Space Sci.* 115, 102–109. [7] R. M. Killen et al. (2018), in *The View after MESSENGER*, 407–429. [8] D. Gamborino et al. (2019) *Ann. Geophys.* 37, 455–470. [9] B. Hapke (2012) *Theory of Reflectance and Emittance Spectroscopy*. [10] C. D. Moak et al. (1959) *Rev. Sci. Instrum.* 30, 694–699. [11] D. G. Seely et al. (2008) *Nucl. Instrum. Methods A* 585, 69–75.